

4.7.5 Infilled discontinuities

- (c) The shear stress--displacement curves of filled discontinuities often have two portions, the first reflecting the deformability of the filling materials before rock to rock contact is made, and the second reflecting the deformability and shear failure of rock asperities in contact.
- (d) The shear strength of a filled discontinuity does not always depend on the thickness of the filling. If the discontinuity walls are flat and covered with a low-friction material, the shear surface will be located at the filling-rock contact.
- (e) Swelling clay is a dangerous filling material because it loses strength on swelling and can develop high swelling pressures if swelling is inhibited.

4.8 Models of discontinuity strength and deformation

4.8.1 The Coulomb friction, linear deformation model

The simplest coherent model of discontinuity deformation and strength is the Coulomb friction, linear deformation model illustrated in Figure 4.45.

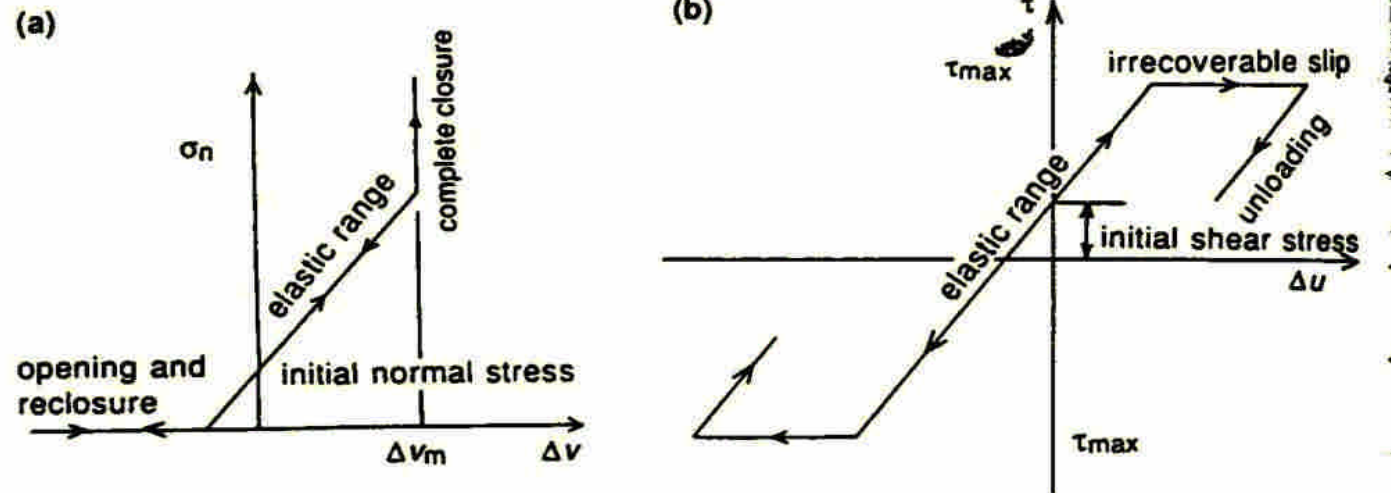


Figure 4.45 Coulomb friction, linear deformation joint model; (a) normal stress (σ_n)–normal closure (Δv) relation; (b) shear deformation (τ)–shear displacement (Δu) relation.

4.8.2 The Barton-Bandis model

The Barton-Bandis discontinuity closure model incorporates hyperbolic loading and unloading curves (Figure 4.46a)

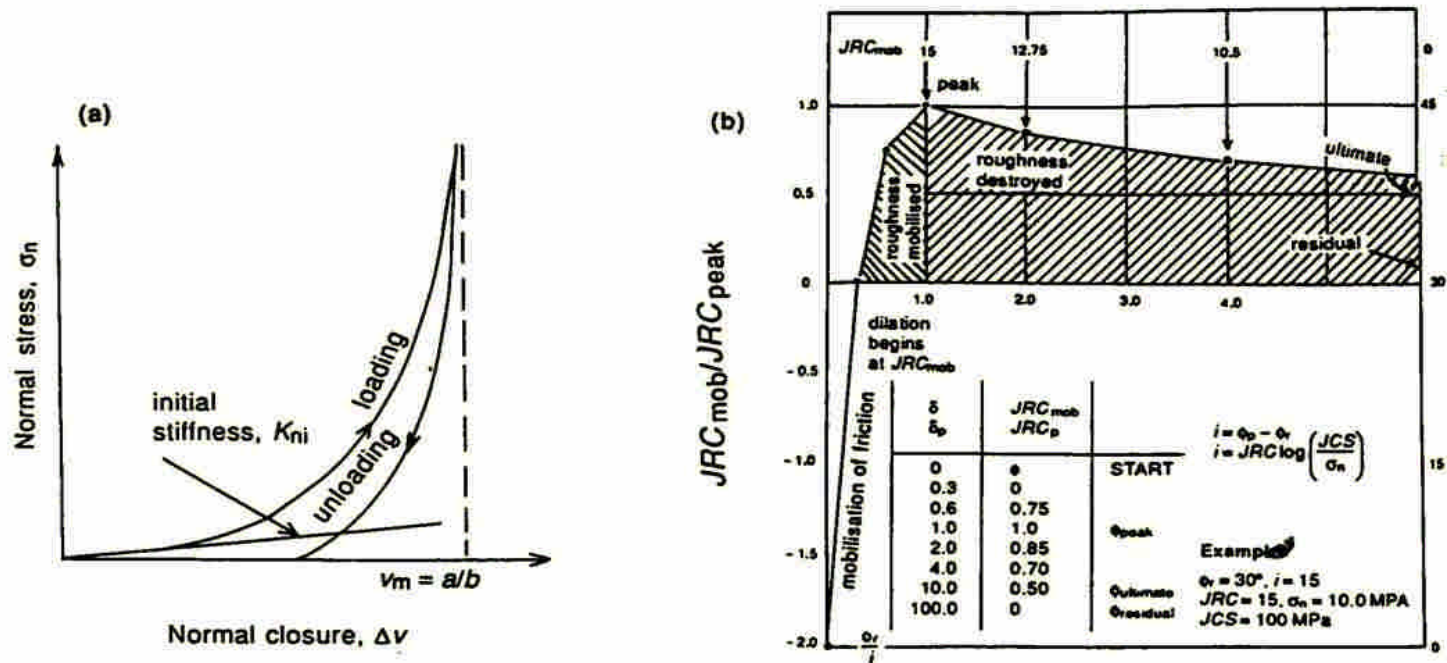


Figure 4.46 The Barton-Bandis model: (a) normal stress-normal closure relation; (b) example of piecewise linear shear deformation simulation (after Barton *et al.*, 1985).

4.8.2 The Barton-Bandis model

In which normal stress and closure, Δv , are related by the empirical expression 課本有誤

$$\sigma_n = \Delta v / (a - b\Delta v) \quad (4.35)$$

where a and b are constants. The initial normal stiffness of the joint, K_{ni} , is equal to the inverse of a and the maximum possible closure, v_m , is defined by the asymptote a/b .

4.8.2 The Barton-Bandis model

Differentiation of equation 4.35 with respect to Δv yields the expression for **normal stiffness**

$$K_n = K_{ni} \left[1 - \sigma_n / (v_m K_{ni} + \sigma_n) \right]^{-2}$$

- Bandis et al. (1985) present the empirical relations

$$K_{ni} = 0.02(JCS_0 / E_0) + 2.0 JRC_0 - 10$$

$$v_m = A + B(JRC_0) + C(JCS_0 / E_0)^D$$

where JCS_0 and JRC_0 are laboratory scale values, E_0 is the initial aperture of the discontinuity, and A , B , C and D are constants which depend on the previous stress history.

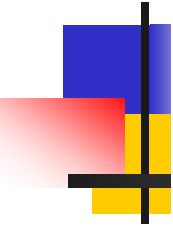
4.8.2 The Barton-Bandis model

The Barton-Bandis model takes explicit account of more features of discontinuity strength and deformation

behaviour than the elementary model discussed


- in section 4.8.1. However, its practical application may present some difficulties. In particular, the derivation of relations for the mobilisation and degradation of surface roughness from a piecewise linear graphical format rather than from a well-behaved formal expression may lead to some irregularities in numerical simulation of the stress-displacement behaviour.

4.8.3 The continuous-yielding joint model



The continuous-yielding joint model was designed to provide a coherent and unified discontinuity deformation and strength model, taking account of non-linear compression, non-linearity and dilation in shear, and a non-linear limiting shear strength criterion. Details of the formulation of the model are given by Cundall and Lemos (1988).

4.8.3 The continuous-yielding joint model



The key elements of the model are that all shear displacement at a discontinuity has a component of plastic (irreversible) displacement, and all plastic displacement results in progressive reduction in the mobilised friction angle. The displacement relation is

$$\Delta u^p = (1 - F) \Delta u$$

where Δu is an increment of shear displacement, Δu^p is the irreversible component of shear displacement and F is the fraction that the current shear stress constitutes of the limiting shear stress at the prevailing normal stress.

The progressive reduction in shear stress is represented by

$$\Delta \phi_m = -\frac{1}{R} (\phi_m - \phi) \Delta u^P$$

where ϕ_m is the prevailing mobilised friction angle, ϕ is the basic friction angle, and R is a parameter with the dimension of length, related to joint roughness.

The response to normal loading is expressed incrementally as

$$\Delta \sigma_n = K_n \Delta v$$

where the normal stiffness K_n is given by

$$K_n = \alpha_n \sigma_n^{\beta_n}$$

in which α_n and β_n are model parameters.

4.8.3 The continuous-yielding joint model

The shear stress and shear displacement increments are related by

$$\Delta\tau = FK_s\Delta u$$

where the shear stiffness may also be taken to be a function of normal stress, e.g.

$$K_s = \alpha_s \sigma_n^{\beta_s}$$

in which α_s , β_s are further model parameters.

4.9 Behaviour of discontinuous rock masses

4.9.1 Strength

The determination of the **global mechanical properties** of a

large mass of discontinuous in situ rock remains one of the

most difficult problems in the field of rock mechanics.

The sets of discontinuities are mutually inclined at 45° as shown in the sketches in Figure 4.47.

4.9 Behaviour of discontinuous rock masses

4.9.1 Strength

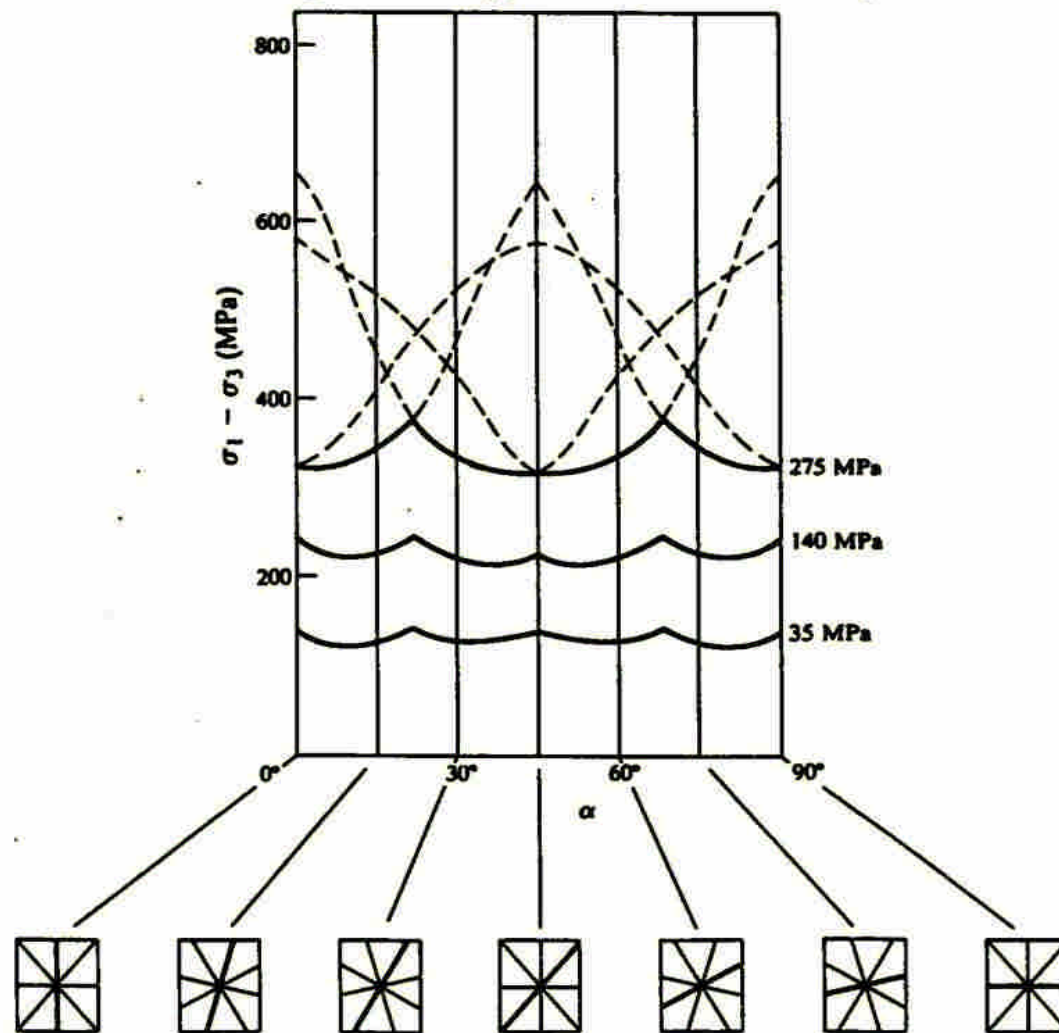



Figure 4.47 Composite peak strength characteristics for a hypothetical rock mass containing four sets of discontinuities each with the properties of the cleavage in the slate for which the data shown in Figure 4.31b were obtained.

4.9 Behaviour of discontinuous rock masses

4.9.1 Strength



A curve showing the variation of the peak principal stress difference with the orientation angle, α , may be constructed for a given value of σ_3 by

superimposing four times the appropriate curve in Figure 4.31 b with each curve displaced from its neighbour by 45° on the α axis. Figure 4.47 shows the resulting rock mass strength characteristics for three values of σ_3 . In this case, failure always takes place by slip on one of the discontinuities.

4.8.3 The continuous-yielding joint model

The most completely developed of these empirical approaches is that introduced by Hoek and Brown (1980) who proposed the empirical rock mass strength criterion

$$\sigma_{1s} = \sigma_3 + (m \sigma_c \sigma_3 + s \sigma_c^2)^{1/2} \quad (4.36)$$


Hoek and Brown (1980) showed that their criterion could also be expressed in terms of shear strength, τ , and normal stress, σ_n , as

$$\tau_n = A(\sigma_n - \sigma_{tn})^B$$

$$\tau_n = \tau / \sigma_c \quad \sigma_n = \sigma_n / \sigma_c \quad \sigma_{tn} = \left[\frac{1}{2} m - (m^2 + 4s)^{1/2} \right] \sigma_c \quad (4.37)$$

Hoek and Brown (1988) proposed a revised set of relations between Bieniawski's rock mass rating (RMR) and the parameters m and s :

Disturbed rock masses


$$\frac{m}{m_i} = \exp\left(\frac{RMR - 100}{14}\right)$$

$$s = \exp\left(\frac{RMR - 100}{6}\right) \quad (4.39)$$

Undisturbed or interlocking rock masses

$$\frac{m}{m_i} = \exp\left(\frac{RMR - 100}{28}\right) \quad (4.40)$$

$$s = \exp\left(\frac{RMR - 100}{9}\right) \quad (4.41)$$

where m_i is the value of m for the intact rock as given in section 4.5.4.

4.9 Behaviour of discontinuous rock masses

4.9.1 Strength

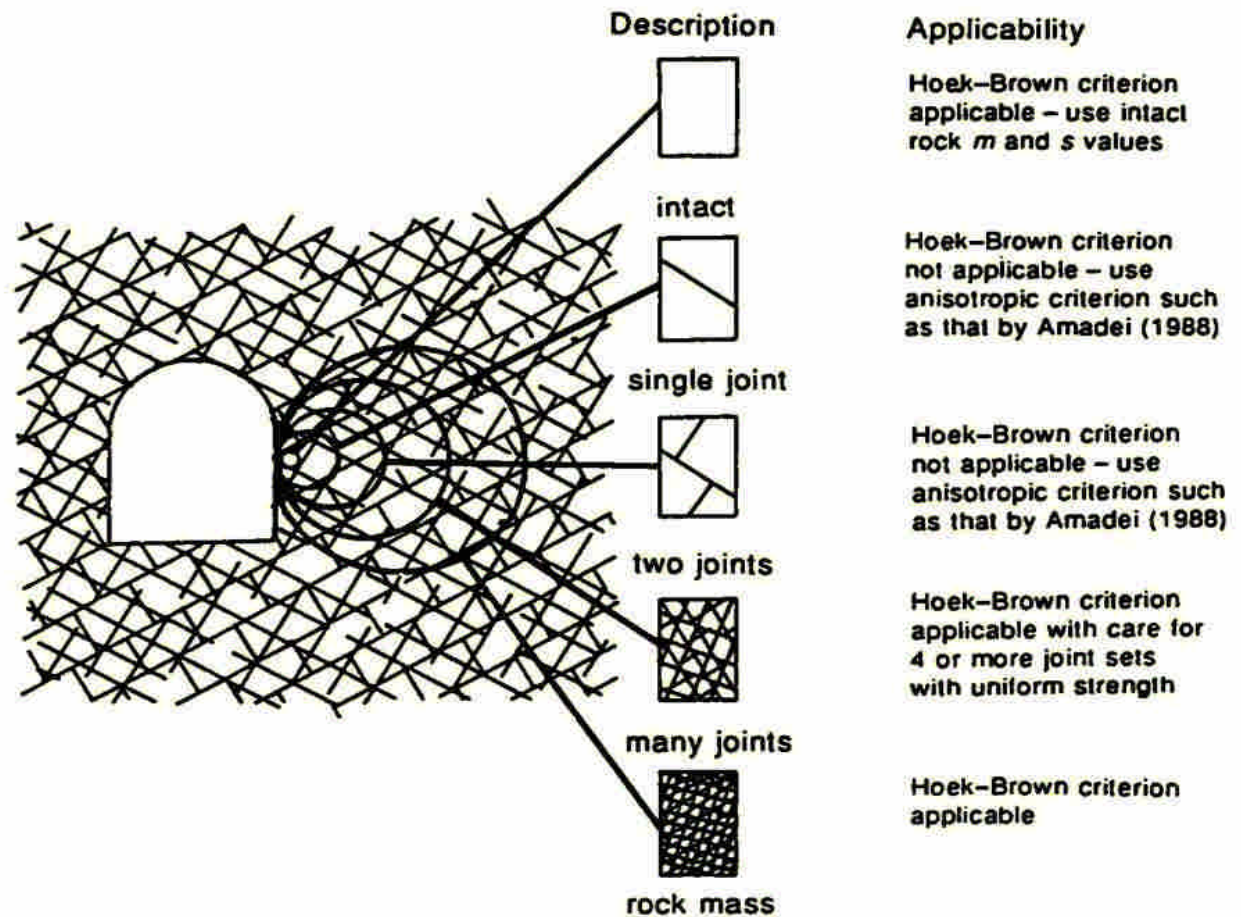


Figure 4.48 Applicability of the Hoek-Brown empirical rock mass strength criterion at different scales (after Hoek and Brown, 1988).

4.9 Behaviour of discontinuous rock masses

4.9.1 Strength

Figure 4.49 shows an example of the application of **Hoek and Brown's criterion** to a **sandstone rock mass** at the site of a proposed underground excavation. Triaxial compression tests on samples of intact sandstone gave the upper envelope with $m_i = 15$. Logging of the cores showed that the rock mass rating varied from **65 (good) to 44 (fair)**. For a sandstone rock mass in the **undisturbed or interlocked condition**, equations 4.40 and 4.41 give $m = 4.298$, $s = 0.0205$ for $RMR = 65$ and $m = 2.030$, $s = 0.0020$ for $RMR = 44$. These values, used in conjunction with a mean value of $\sigma_c = 35 \text{ MPa}$, give the estimated bounds to the in situ rock mass strength, shown in Figure 4.49.

4.9 Behaviour of discontinuous rock masses

4.9.1 Strength

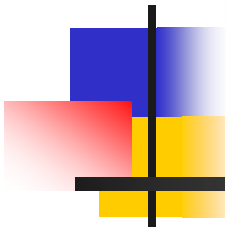
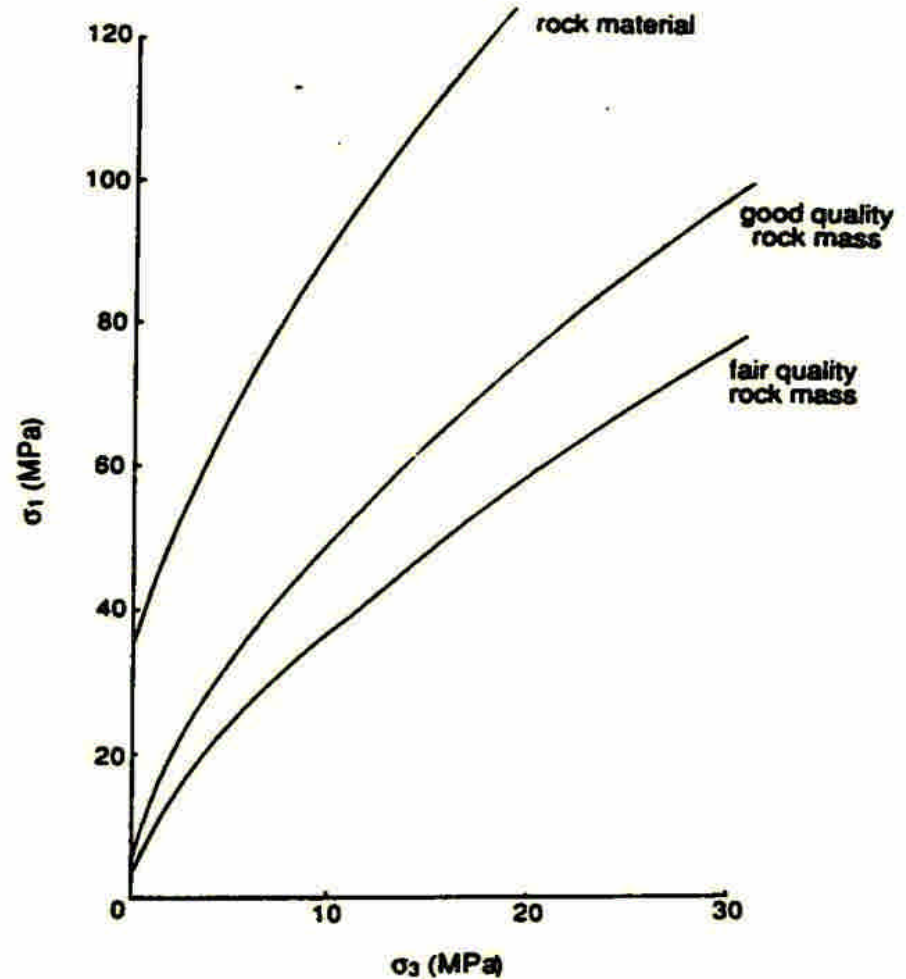


Figure 4.49 Hoek–Brown rock mass strength criterion applied to a sandstone rock mass with $\sigma_c = 35$ MPa.



4.9.2 Deformability

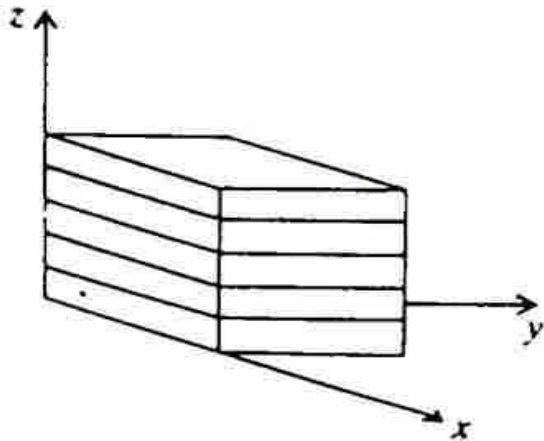


Figure 2.10 A transversely isotropic body for which the x, y plane is the plane of isotropy.

In the simplest case of a rock mass containing a single set of **parallel discontinuities**, a set of elastic constants for an **equivalent transversely isotropic continuum** may be determined. For a case analogous to that shown in Figure 2.10, let the rock material be isotropic with elastic constants E and ν , let the discontinuities have **normal and shear stiffnesses** K_n and K_s as defined in section 4.7.5, and let the **mean discontinuity spacing** be S .

4.9.2 Deformability

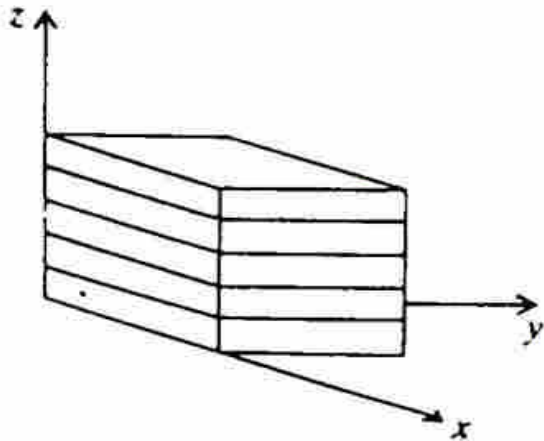


Figure 2.10 A transversely isotropic body for which the x, y plane is the plane of isotropy.

By considering the deformations resulting from the application of unit shear and normal stresses with respect to the x, y plane in Figure 2.10, it is found that the equivalent elastic constants required for use in equation 2.42 are given by

$$E_1 = E \qquad \nu_1 = \nu \qquad \nu_2 = \frac{E_2}{E} \nu$$

$$\frac{1}{E_2} = \frac{1}{E} + \frac{1}{K_n S} \qquad \frac{1}{G_2} = \frac{1}{G} + \frac{1}{K_s S}$$

4.9.2 Deformability

If, for example, $E = 10 \text{ GPa}$, $\nu = 0.20$, $K_n = 5 \text{ GPa m}^{-1}$
 $K_s = 0.1 \text{ GPa m}^{-1}$ and $S = 0.5 \text{ m}$,

then $G = 4.17 \text{ GPa}$, $E_1 = 10 \text{ GPa}$, $E_2 = 2.0 \text{ GPa}$,

$\nu_1 = 0.20$, $\nu_2 = 0.04$ and $G_2 = 49.4 \text{ MPa}$.

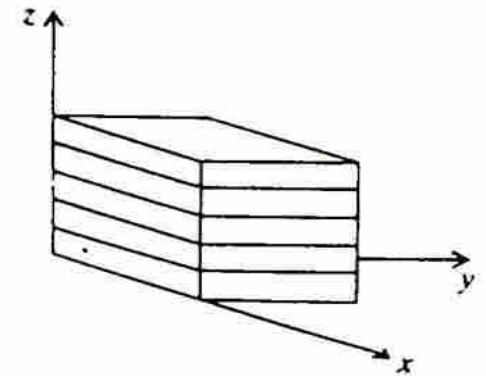


Figure 2.10 A transversely isotropic body for which the x, y plane is the plane of isotropy.

4.9.2 Deformability

Using a simple analytical model, Brady et al. (1985) have demonstrated that, in this case:

- (a) the loading-unloading cycle must be accompanied by hysteresis; and
- (b) it is only in the initial stage of unloading (Figure 4.50) that inelastic response is suppressed and the true elastic response of the rock mass is observed.

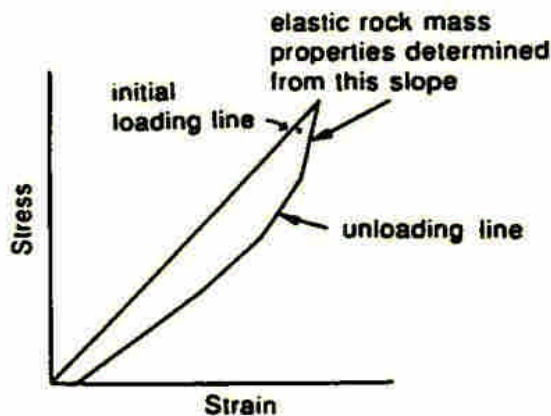


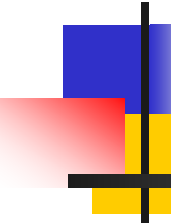
Figure 4.50 Determination of the Young's modulus of a rock mass from the response on initial unloading in a cyclic loading test (after Brady *et al.*, 1985).

4.9.2 Deformability

Bieniawski (1978) compiled values of **in situ modulus of deformation** determined using a range of test methods at 15 different locations throughout the world. He found that for values of rock mass rating, **RMR, greater than about 55**, the mean deformation modulus, E_M , measured in GPa, could be approximated by the empirical equation

$$E_M = 2(RMR) - 100 \quad (4.42)$$

4.9.2 Deformability



Serafim and Pereira (1983) found that an improved fit to their own and to Bieniawski's data, particularly in the range of E_M between 1 and 10 GPa, is given by the relation

$$E_M = 10^{\frac{RMR - 10}{40}} \quad (4.43)$$